

Estimating the correlation between operational risk loss categories over different time horizons

Maurice L. Brown ; Cheng Ly[†]

Abstract

Operational risk is challenging to quantify because of the broad range of categories (fraud, technological issues, natural disasters) and the heavy-tailed nature of realized losses. Operational risk modeling requires quantifying how these broad loss categories are related. We focus on the issue of loss frequencies having different time scales (e.g., daily, yearly, monthly basis), specifically on estimating the statistics of losses on arbitrary time horizons. We present a frequency model where mathematical techniques can be feasibly applied to analytically calculate the mean, variance, and co-variances that are accurate compared to more time-consuming Monte Carlo simulations. We show that the analytic calculations of cumulative loss statistics in an arbitrary time window are feasible here and would otherwise be intractable due to temporal correlations. Our work has potential value because these statistics are crucial for approximating correlations of losses via copulas. We systematically vary all model parameters to demonstrate the accuracy of our methods for calculating all first and second order statistics of aggregate loss distributions. Finally, using combined data from a consortium of institutions, we show that different time horizons can lead to a large range of loss statistics that can significantly affect calculations of capital requirements.

1 Introduction

It is imperative to properly quantify risk (Jiřina, 2011) since it drives financial behavior. A particularly challenging risk type to model is Operational Risk, defined as the risk of loss resulting from inadequate or failed internal processes, people or systems, or from external events (Bank For International Settlements, 2014). Traditionally, operational risk has been neglected compared to credit and market risk; it is often thought of as “other” despite how it has severely harmed institutions when not properly accounted for (Bank For International Settlements, 2014; Chernobai et al., 2008). For example, in the last few decades operational losses have been extraordinary, leading to wholesale changes for many institutions in the form of bankruptcies, mergers, re-organizations, and other lasting damage (Chernobai et al., 2008; De Fontnouvelle et al., 2003). The major sources of operational risk include IT security, over reliance on suppliers, integration of acquisitions, fraud, error, customer service quality, alleged wrongdoing in business practices (Afonso et al., 2019), regulatory compliance, recruitment, training and retention of staff, and social and environmental impacts (Bank For International Settlements, 2014). Operational risk loss data are used in models to calculate statistics that aid in decision making for the size of capital reserves but also to make predictions to mitigate and understand the dynamics of operational losses.

Operational risk is important because it has accounted for a large proportion of losses (Afonso et al., 2019), especially for the largest institutions. Quantifying it presents unique mathematical and statistical challenges stemming from the broad range of risk categories, heavy-tailed data, as well as lack of data for certain categories (e.g., Disasters and Public Safety, Technology and Infrastructure Failure, see Table 2). Moreover, losses in different categories occur with different frequency time-scales, ranging from a daily, monthly, or yearly basis. There are many global factors (business cycle, pandemics, wars, etc.) that impact multiple loss categories, leading to correlations between different categories of losses.

There are risk categories where the data is scarce and commonly used methods to fit a loss distribution model to data would suffer from insufficient sample size. Estimating the correlation between loss categories with scarce data is challenging; the status quo is to calculate a time-averaged correlation/covariance of the loss data in the same time window used in a copula model (McNeil et al., 2015). With scarce data, it is common to use the raw data in shorter time windows (i.e., daily or monthly) to get more samples rather than on cumulative data summed over the desired time window, which should be yearly data since the desire is to calculate yearly capital (Chernobai et al., 2008). Thus, we focus on how different time horizons of losses potentially impact loss statistics.

Shedding light on how loss statistics (for a specific category and between different categories) depend on time horizons, or **time windows**, naturally leads to focussing on the frequency distribution. We introduce a stochastic point process model for the frequency distribution that has two main parameters: average frequency and a time scale parameter. The advantages of this model are as follows: i) the parameters could be fit with sufficient data but are also transparent enough to understand when fitting to scarce data, ii) when coupled with an independent severity distribution model, the auto- and cross-correlation functions are mathematically tractable, so we can analytically calculate the cumulative loss statistics over varying time windows using tools from signal processing (Kay, 1993) and computational neuroscience (Lindner et al., 2005; Shea-Brown et al., 2008; Barreiro and Ly, 2017, 2018). Varying all model parameters, we show the advantages and shortcomings of our calculations compared to large-scale Monte Carlo simulations. Finally, using combined data from a consortium of institutions, we fit our model to loss statistics of an average institution. We show that different time windows of (cumulative) losses can lead to a large range of loss statistics, which in turn can significantly effect calculations of capital requirements.

2 Results

A central Operational Risk Modeling objective is to estimate the cumulative loss distribution because the 99.9 percentile of this is a common capital requirement (Jirina, 2011). Operational losses are realizations of a continuous stochastic process from both a frequency distribution (event occurrences) and severity distribution (amount of loss) (Jirina, 2011). The Basel II Committee has suggested several approaches to calculate the capital requirements to withstand exposure to operational risk, with varying levels of sophistication: (1) Basic Indicator Approach, (2) Standardized Approach and (3) Advanced Mea-

surement Approaches (**AMA**) (Bank For International Settlements, 2014; Chernobai et al., 2008). Among the 3 approaches, the AMA is the required approach for large institutions (Bank For International Settlements, 2014) and known to be the most risk sensitive compared to the other 2 approaches that are often used for smaller institutions (Bank For International Settlements, 2014; Chernobai et al., 2008). Here we will only focus on the AMA because it is used for larger banks that tend to suffer larger operational losses, and requires the most complex mathematical and statistical methods. Our proposed methods could potentially address the shortcomings of the AMA we discussed in the Introduction.

The broad operational loss categories naturally have different time scales for frequency of events as well as different loss amounts (severity). The AMA approach entails modeling both the frequency and severity distributions, and ultimately combined into a single **aggregate loss distribution** for a given operational loss category (Chernobai et al., 2008). The severity distributions, are often modeled by parametric distributions of positive random variables that are heavy-tailed; e.g., lognormal, Weibull, Pareto and Burr (Chernobai et al., 2008). The frequency distribution is commonly modeled with a Poisson Process or the negative binomial distribution (Chernobai et al., 2008).

Our main focus is on frequency distribution modeling because our aim is to show how inappropriately processing data in time can lead to unexpected results. Indeed, a simple example in Fig 1 shows how the time window of cumulative losses can dramatically alter the loss distribution statistics. The convention we use throughout is that the dark blue denotes losses in a small time window Δt , light blue denotes losses in a larger time window T_w . The actual loss time series is R , and cumulative losses in window T_w is Q .

The outline of the paper is as follows:

- Describe and analyze the Inhomogeneous Poisson Process frequency distribution model for single loss time series.
- Develop theory for capturing statistics of cumulative losses in arbitrary time windows.
- Extend Inhomogeneous Poisson Process model to multiple loss time series, allowing input correlations in frequency distribution and heterogeneity across risk categories. Derive formulas for covariance of loss distributions in arbitrarily large time windows.
- Apply theory to data averages obtained from consortium to demonstrate why careful consideration of time windows for loss reporting is necessary.

Background assumptions

The loss distribution model consists of both a frequency and a severity distribution for a given operational risk loss categories (Bank For International Settlements, 2014; Chernobai et al., 2008). To enable mathematical analysis, we make two common assumptions: the time series is stationary (i.e., the statistics do not vary over time), and that frequency is independent of severity (Bank For International Settlements, 2014; Chernobai et al., 2008). That is:

$$\mu(t_0) = \mu(t_1) = \mu_X. \tag{1}$$

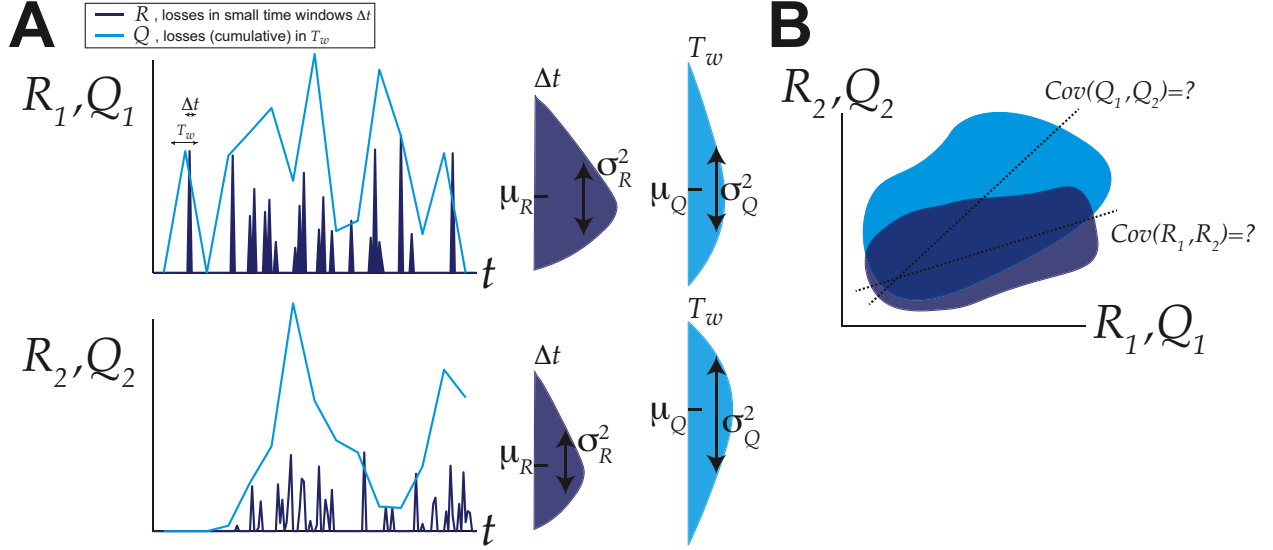


Figure 1: **Operational risk loss statistics can vary depending on risk category and on time window of observations.** **A)** Examples of two different loss time series (top and bottom). For each loss category, two time series from the same loss data are shown: losses in small windows (Δt dark blue) which are denoted by $R_j(t)$ and cumulative losses in time window T_w denoted by $Q_j(t)$. Right panels show aggregate loss distributions averaged over time, labeled with corresponding statistics of interest. **B)** Depictions of the range of the joint distributions of (R_1, R_2) (dark blue) and (Q_1, Q_2) (light blue). The covariance and correlation are important for calculating aggregate capital different risk categories, but can depend on time window of observations.

We let $I(t)$, the frequency distribution, indicate whether a loss event occurred at time t

$$I(t) = \begin{cases} 0, & \text{no loss event at time } t \\ 1, & \text{have loss event at time } t. \end{cases} \quad (2)$$

Let S denote the random size of the loss (severity). The loss time series $R(t)$ is:

$$R(t) = I(t) * S \quad (3)$$

The independence assumption is:

$$f_{I,S} = f_I * f_S \quad (4)$$

where f_X denotes the marginal distribution (PDF) of $X \in \{I, S\}$.

Note that time t is theoretically continuous, loss events occur at discrete time points as a point process, and loss magnitudes S are continuous. However, since the model is represented on a computer, we use discrete time (Δt). The resulting formulas presented here account for time step length Δt to make a direct correspondence with our publicly available computer code, and should thus be more useful to other practitioners.

2.1 Time series with inhomogeneous Poisson Process frequency distribution

Realistic models of loss frequencies must account for (time-)dependence between loss events; operations of institutions are not simply memory-less like an homogeneous Poisson Process. Here we include time-varying dynamics via an inhomogeneous Poisson Process model, where the probability of $R(t) > 0$ depends on time. Throughout the rest of the paper, we will refer to standard methods used to calculate loss statistics for a simple homogeneous Poisson Process model for the frequency distribution, which are provided in Appendix 5A. Note that the resulting loss time series when the frequency distribution is a Poisson Process is commonly referred to as a marked Poisson Process (Last and Penrose, 2017) where the mark is a continuous positive random variable corresponding to the severity.

The direct calculation of the (co-)variance of cumulative losses in larger windows T_w is unwieldy because of the large number ($\binom{n}{2}$ where n is the number of observations in T_w) of different $R_j R_k$ correlated terms, and the distribution of the number of loss events is generally intractable with temporal correlations. We use an approximation to relate the autocovariance $A(t)$ to the variance of cumulative losses in time window T_w (Kay, 1993; Shea-Brown et al., 2008; Litwin-Kumar et al., 2011, 2012; Barreiro and Ly, 2017, 2018):

$$\sigma_Q^2 = \int_{-T_w}^{T_w} A(t) (T_w - |t|) dt \quad (5)$$

because the autocovariance $A(t)$ is tractable (this formula assumes $A(t)$ is sufficient for calculating σ_Q^2 , see Materials and methods section for details).

Here $R(t) = S * I(t)$, with $P(I(t) = 1) = \nu(t)\Delta t$ where the time points t are spaced a part by Δt , and where $\nu(t)$ is the probability per unit time of a loss event occurring. We assume $\nu(t)$ is governed by a stochastic differential equation:

$$\tau \frac{d}{dt} \nu(t) = -\nu(t) + \tau a \sum_k \delta(t - t_k) \quad (6)$$

where t_k are random points drawn from a homogeneous Poisson Process with rate γ , a is the jump size of $\nu(t)$ at times t_k , and τ is the time-scale that determines how fast $\nu(t)$ decays to 0 in the absence of random jumps at t_k . The dynamics are essentially determined by two main factors: (γ, a) controls the magnitude of increases in frequency, and τ is a measure of the memory (larger values correspond to longer memory). In contrast to some other time series models, this stochastic differential equation formulation consists of parameters that are easy to understand: magnitude and memory or time-scale. This frequency model (Eq.(6)) is a simple generalization of a homogeneous Poisson Process, seen by taking the limit $\tau \rightarrow 0$, $a \rightarrow \infty$ so that $a\tau = 1$. This model has not been precisely calibrated to data (but see application to data below). The model is very similar in form to a Hawkes process (Hawkes, 1971, 2018) commonly used in finance and numerous applications; it is a point process model where the probability rate of an event (randomly) changes at prescribed points and could be followed by exponential decay.

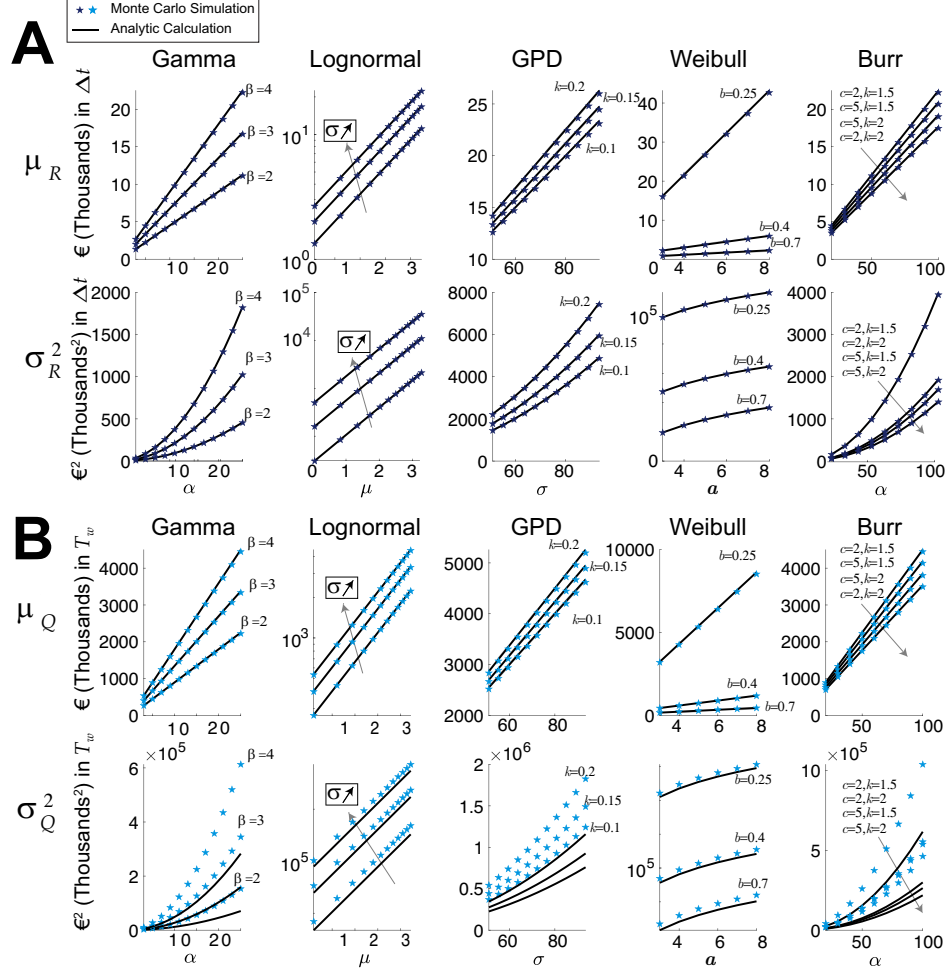


Figure 2: **Validation of results for inhomogeneous Poisson Process frequency model (6).** Comparing mean and variance of aggregate loss time series with inhomogeneous Poisson Process frequency distribution (here we set $\tau = 1.2, a = 1, \gamma = 75/2$) for common severity distributions (see Table 3). Note that Table 2 shows that this average frequency is typical in industry-wide reporting. **A)** Comparing the analytic formula for μ_R (Eq.(27)), σ_R^2 (Eq.(32)) (solid lines) with the Monte Carlo simulations (stars), and similarly for Q in **(B)**: μ_Q (Eq.(33)), and σ_Q^2 (Eq.(35)), with $\Delta t = 0.001$ in time units of years (≈ 0.365 day). For Lognormal, $\sigma = \sqrt{2 \log(2)}, \sqrt{2 \log(3)}, \sqrt{2 \log(4)}$; ; vertical axis is log-scale for Lognormal, and Weibull variance. The results for σ_Q^2 are not as accurate, but the general trends are captured (see Fig. 3A) The Monte Carlo simulations are for 50,000 realizations with each times series 100 years long. The severity distribution parameters vary greatly because we perform a large parameter sweep, but the average is about 10 to 100 € per loss event, so that average yearly loss is on the order of 10s of millions of €, consistent with industry reporting (Table 2).

We are interested in the statistics of the loss time series $R_j(t)$ and $Q_j(t)$, including the mean μ_R and variance σ_R^2 in both small time windows and arbitrarily large windows T_w : μ_Q , σ_Q^2 . Thus we derive analytic formulas for these entities (see Materials and methods section (Eq (27), (32), (33), (35); black lines in Fig 2)); we also state the corresponding entities for the frequency distribution ($\nu(t)$ and \mathcal{V} for sum of events in T_w) that will be instrumental in fitting our model to data:

$$\begin{aligned}
\mathbb{E}[\nu(t)] &= a\tau\gamma \\
Var(\nu(t)) &= \frac{a^2\gamma\tau}{2} \\
\mathbb{E}[\mathcal{V}] &= T_w a\gamma\tau \\
Var(\mathcal{V}) &= a^2\gamma\tau^2(T_w + \tau(e^{-T_w/\tau} - 1)) \\
\mu_R &= \mu_S(a\gamma\tau\Delta t) \\
\sigma_R^2 &= \mu_{S^2}(a\tau\gamma\Delta t) - (\mu_S a\tau\gamma\Delta t)^2 \\
\mu_Q &= T_w a\gamma\tau\mu_S \\
\sigma_Q^2 &= 2\frac{\sigma_R^2}{\Delta t}\tau(T_w + \tau(e^{-T_w/\tau} - 1))
\end{aligned}$$

These formulas are generally very accurate in comparison to the Monte Carlo simulations (stars, Fig 2). The glaring exception is the analytic approximation of σ_Q^2 in Fig 2B (bottom row, black lines); our theory does not accurately capture the Monte Carlo simulations (light blue stars).

Explanation of σ_Q^2 mismatch: This was initially surprising to us, previously believing that there might have been an error in our analytic calculation and/or in the Monte Carlo simulations. After much investigation and careful re-checking, we are certain that this quantitative mismatch is not easily rectifiable in these operational risk models. Indeed, others have found there can be discrepancies with simulations and this same calculation (Eq. (35)) to approximate statistics in different time windows. Although the details of the models are different, we see this in the variance/covariance of (spike) statistics in many other contexts (e.g., see Fig 2C, Fig 5B, Fig 6B2 in Litwin-Kumar et al. (2012), Fig 3B,C,D in Litwin-Kumar et al. (2011), Fig 2 in Barreiro and Ly (2017)); the important trends are captured by the formula but there is not precise quantitative matches to Monte Carlo simulations.

Our analytic calculation still has value in capturing the qualitative trends of the Monte Carlo simulations. A simple scalar factor can yield relatively accurate approximations (Fig 3), indicating that our formula

$$\sigma_Q^2 = 2\frac{\mu_{S^2}(a\tau\gamma\Delta t) - (\mu_S a\tau\gamma\Delta t)^2}{\Delta t}\tau(T_w + \tau(e^{-T_w/\tau} - 1)) \quad (7)$$

reveals the relative trends as parameters are varied. Fig 3A shows the comparisons of the analytic theory (black curve) but also with a scaling factor (gray curves); the parameters here

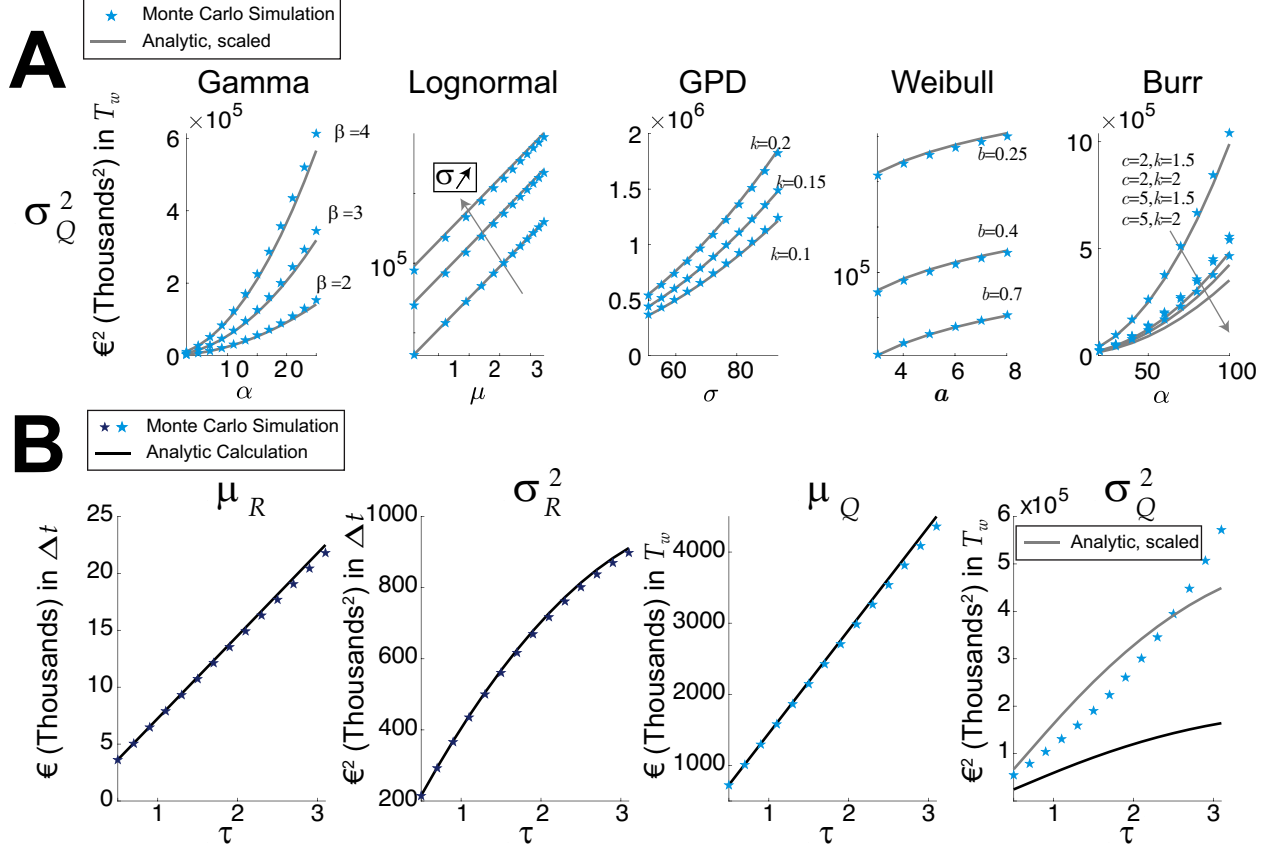


Figure 3: **A simple scale factor can yield accurate results.** Quantitative inaccuracies between the Monte Carlo simulation and the analytic formula (Eq.(35)) for σ_Q^2 are fixed with a single scaling factor. **A)** Same as Figure 2B, except analytic formula are scaled by 2, 1.5, 1.6, 1.5, 1.6, respectively. The scaling factors were manually determined. **B)** Fixing all parameters ($a = 1, \gamma = 75/3.1$) except τ that varies from 0.5 to 3.1 (unit=years), using a Gamma distributed severity distribution $S \sim \text{Gamma}(\alpha = 20, \beta = 3)$; last column has σ_Q^2 scaled by 2.74. The accuracy of the theory slightly diminishes as τ increases.

are the same same parameters as bottom row in Fig 2B). Fig 3B shows how our analytic calculation approximates the statistics as the time-scale of the inhomogeneous frequency distribution, τ , varies; as τ increases there appears to be more discrepancies between the Monte Carlo and the analytic calculations. The last panel on the far-right for σ_Q^2 shows both the original formula (black) and the curve scaled by 2.74 (gray; computed as least-squares fit to the stars).

Technical remark: in Figures 2–3, rather than simulating a realization of a long time series (as in Fig. 11), we simulated many realizations (50,000) of a moderate length time. This was to insure that the autocovariance of $R(t)$, $A_R(t)$ was accurately captured compared to the theory (Eq. (34)); see Figure 4B with 50,000 realizations in red. Note that a very small number of realizations can accurately capture the autocovariance of the time-varying

inhomogeneous Poisson rate $\nu(t)$ (Fig. 4A).

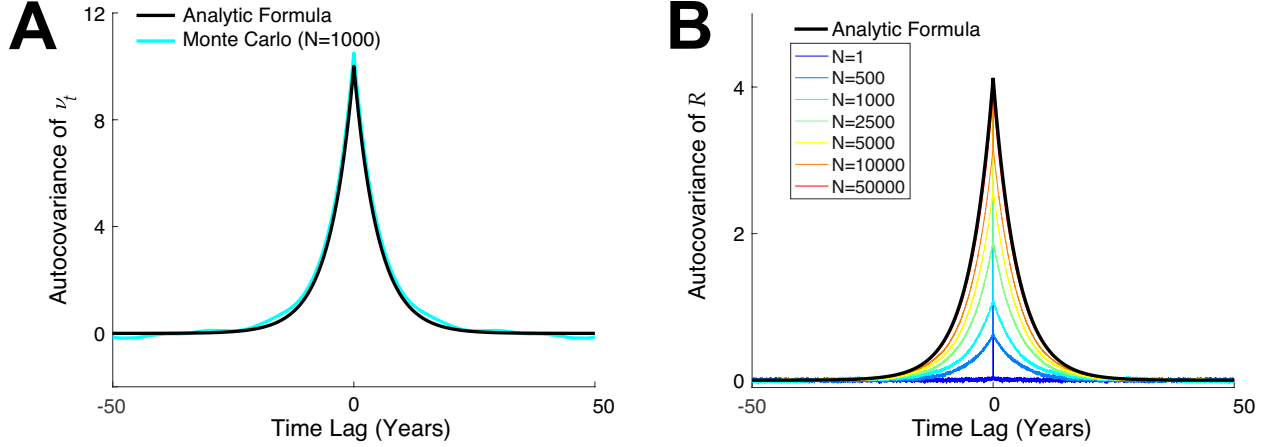


Figure 4: **The number of realizations effects Monte Carlo of $A_R(t)$ significantly.** Consider the inhomogeneous Poisson Process model for the frequency distribution in (31) ($\gamma = 4$ events/year, $a = 1$ event/year, $\tau = 5$ years), with a gamma distribution for the severity $S \sim \text{Gamma}(\alpha = 1.5, \beta = 2.5)$. **A)** Comparison of the auto-covariance of the frequency distribution: $A_{\nu(t)}(t)$, calculated from Monte Carlo simulations (cyan) of Eq. (6) with theoretical calculation (black, from Eq. (31)) shows good agreement with relatively few realizations ($N = 1000$, 1000 years for each realization). **B)** Comparisons of $A_R(t)\Delta t$ calculated from Monte Carlo simulations (rainbow) with theoretical calculation (black, from Eq. (34)) shows that many realizations are required to achieve accuracy.

2.2 Multiple loss time series

We extend the methods for a single loss category to two loss categories, which often suffices for calculating aggregate capital because pairwise correlations are commonly used to determine diversification of risk (Chernobai et al., 2008). Although we assume that the frequency distributions for both loss categories have the same form as Eq. (6):

$$\tau_1 \nu'_1 = -\nu_1 + \tau_1 a_1 \sum_{k_1} \delta(t - t_{k_1}) \quad (8)$$

$$\tau_2 \nu'_2 = -\nu_2 + \tau_2 a_2 \sum_{k_2} \delta(t - t_{k_2}) \quad (9)$$

a key difference is that the frequencies can be correlated. The random times t_{k_1}, t_{k_2} are again governed by an inhomogeneous Poisson Process with rates γ_1 and γ_2 , respectively, but the random times (t_{k_1}, t_{k_2}) can be correlated. The parameter $c \in [-1, 1]$ is a measure of the correlation between t_{k_1}, t_{k_2} ; letting $\bar{\gamma} := \min(\gamma_1, \gamma_2)$, the value $|c|\bar{\gamma}$ is the probability per unit time that ν_1 and ν_2 instantaneously jump at the same time, both in the positive direction if

$c > 0$ and in opposite directions when $c < 0$. The marginal statistics of ν_j , \mathcal{V}_j , R_j and Q_j , for $j \in \{1, 2\}$, are the same as with a single loss time series:

$$\mathbb{E}[\nu_j] = a_j \tau_j \gamma_j \quad (10)$$

$$\text{Var}(\nu_j) = \frac{a_j^2 \gamma_j \tau_j}{2} \quad (11)$$

$$\mathbb{E}[\mathcal{V}_j] = T_w a_j \gamma_j \tau_j \quad (12)$$

$$\text{Var}(\mathcal{V}_j) = a_j^2 \gamma_j \tau_j^2 \left(T_w + \tau_j (e^{-T_w/\tau_j} - 1) \right) \quad (13)$$

$$\mu_{R_j} = \mu_{S_j} (a_j \gamma_j \tau_j \Delta t) \quad (14)$$

$$\sigma_{R_j}^2 = \mu_{S_j}^2 (a_j \tau_j \gamma_j \Delta t) - (\mu_{S_j} a_j \tau_j \gamma_j \Delta t)^2 \quad (15)$$

$$\mu_{Q_j} = T_w a_j \gamma_j \tau_j \mu_{S_j} \quad (16)$$

$$\sigma_{Q_j}^2 = 2 \frac{\sigma_{R_j}^2}{\Delta t} \tau_j \left(T_w + \tau_j (e^{-T_w/\tau_j} - 1) \right). \quad (17)$$

In the Materials and methods section, we derive an equation for $\text{Cov}(Q_1, Q_2)$ that is based on:

$$\text{Cov}(Q_1, Q_2) = \int_{-T_w}^{T_w} CC_R(t) (T_w - |t|) dt. \quad (18)$$

See Eq (41); the result is:

$$\text{Cov}(Q_1, Q_2) = c \bar{\gamma} \mu_{S_1} \mu_{S_2} a_1 a_2 \frac{\tau_1 \tau_2}{\tau_1 + \tau_2} \left[\tau_1 \left(T_w + \tau_1 (e^{-T_w/\tau_1} - 1) \right) + \tau_2 \left(T_w + \tau_2 (e^{-T_w/\tau_2} - 1) \right) \right] \Delta t.$$

Figs 5–6 shows a summary of the components of our analytic theory, which overall is accurate. In all panels of Fig 5, the two severity distributions are fixed with $S_1 \sim \text{GPD}(k = .15, \sigma = 50)$, $S_2 \sim \text{Weibull}(a = 5, b = 0.4)$. Fig5A shows comparisons of the cross-covariance of the rates (ν_1, ν_2) of the 2 different frequency distributions: $CC_\nu(t)$ (cyan is Monte Carlo, black is calculation Eq (37)). Here we show two input correlations $c = \pm 0.7$ (see legend for parameters of Eqs (8)–(9)). The analytic theory tends to underestimate the cross-covariance of the Monte Carlo, a consistent trend that holds for all parameters we considered (see below). Comparisons of cross-covariance of the actual loss time series (R_1, R_2) unsurprisingly shows that more realizations matches the analytic theory (Eq (41), black dashed) better; that is, the red curve is closest to the black-dashed curves than all of the other colors in Fig 5B (two input correlations $c = \pm 0.5$). Fig 5C show the accuracy of our analytical equation for different time windows T_w for a fixed $c = 0.25$. Finally, Fig 5D shows comparisons for $\text{Cov}(R_1, R_2)$ and $\text{Cov}(Q_1, Q_2)$ with $T_w = 1$ year and $T_w = 2$ years, varying the input correlation c over a large range of values. The theory performs much better with positive input correlation than negative.

Fig 6 has more demonstrations of the analytic theory for covariance of cumulative losses. We vary the input correlation c (see legend for coloring) and randomly choose the severity distribution parameters, which are all independent uniform distributions with the same ranges as in Fig 2 (and Fig 11 in Appendix A). The horizontal axes is the Monte Carlo, vertical is the analytic theory; the diagonal line is solid black, so perfect accuracy are points that

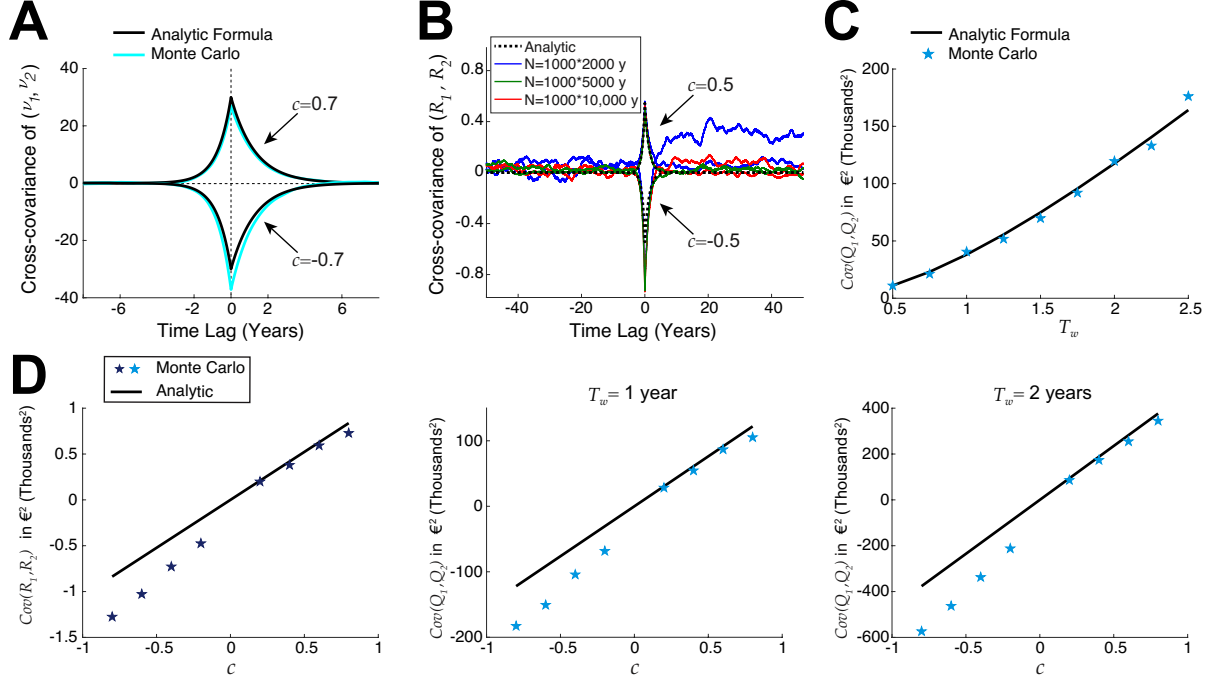


Figure 5: **Analytic theory capture covariance of cumulative losses in different time windows.** **A)** Comparisons of cross-covariance of frequency rates $(\nu_1, \nu_2), CC_\nu(t)$; Monte Carlo (cyan) with very few realizations and analytic theory in solid black (Eq (37)) with input correlations $c = \pm 0.7$. **B)** Comparisons of cross-covariance function of actual loss time series $CC_R(t)$; Monte Carlo in colors with fixed $N = 1000$ but total time 2000 years (blue), 5000 years (red), 10,000 years (green) and analytic theory (black, Eq (41)), with input correlations $c = \pm 0.5$. **C)** Comparisons for $Cov(R_1, R_2)$ and $Cov(Q_1, Q_2)$ with $T_w = 1$ year (middle) and $T_w = 2$ years (right), same format as before. The input correlation c varies across a wide-range. **D)** Varying time windows T_w for a fixed $c = 0.25$. The fixed parameters are: $a_1 = 1.5, \tau_1 = 1.3$ years, $\gamma_1 = 30$ years $^{-1}$, $a_2 = 2, \tau_2 = 0.75$ years, $\gamma_2 = 40$ years $^{-1}$; $S_1 \sim \text{GPD}(k = .15, \sigma = 50)$, $S_2 \sim \text{Weibull}(a = 5, b = 0.4)$.

lie on the diagonal. A–B shows severity: $S_1 \sim \text{Lognormal}$, $S_2 \sim \text{GPD}$; C–D shows severity: $S_1 \sim \text{Weibull}$, $S_2 \sim \text{Burr}$, where Δt windows are shown in A,C and $T_w = 1$ year is shown in B,D. Once again, positive input correlations (reddish) result in better matches than negative (bluish).

Recall that the (point-wise) covariance of the frequency distributions is:

$$Cov(\nu_1, \nu_2) = c\bar{\gamma}a_1a_2 \frac{\tau_1\tau_2}{\tau_1 + \tau_2}. \quad (19)$$

Note that $Cov(\nu_1, \nu_2)$ in larger time windows T_w is:

$$c\bar{\gamma}a_1a_2 \frac{\tau_1\tau_2}{\tau_1 + \tau_2} \left[\tau_1 \left(T_w + \tau_1 (e^{-T_w/\tau_1} - 1) \right) + \tau_2 \left(T_w + \tau_2 (e^{-T_w/\tau_2} - 1) \right) \right]. \quad (20)$$

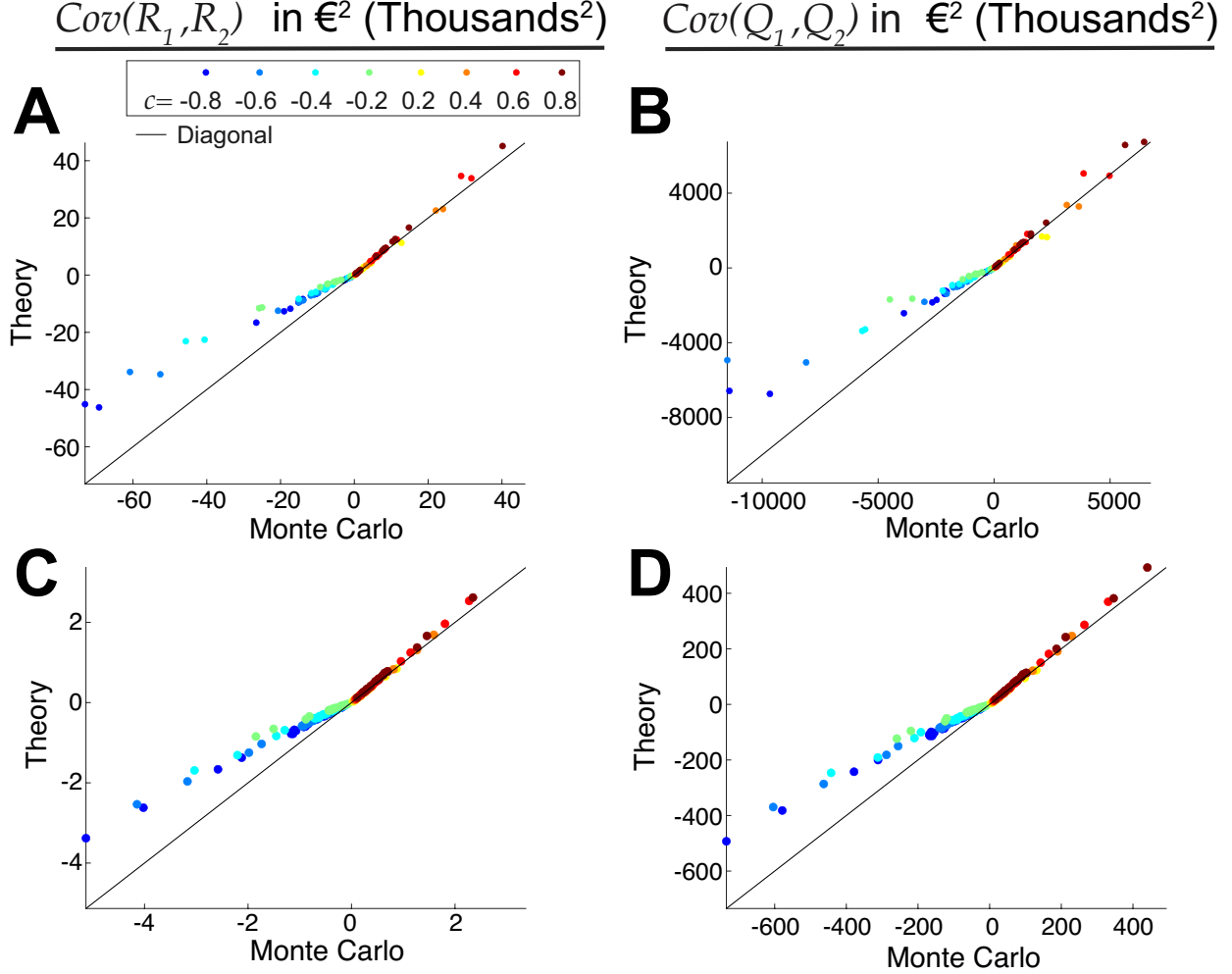


Figure 6: **Analytic theory for covariance of cumulative losses is accurate for random parameters.** Here we set $T_w = 1$ year in **B,D**, but we vary the input correlation c (see legend for coloring), with 20 randomly chosen severity distribution parameters for each c ; severity parameters are all uniform distributions (independent) with the same ranges as in Figs 2,11. The horizontal axes is the Monte Carlo, vertical is the analytic theory; the diagonal line is solid black, so perfect accuracy are points that are on the black line. **A)–B)** $S_1 \sim \text{Lognormal}$, $S_2 \sim \text{GPD}$, with Δt windows (**A**) and $T_w = 1$ year (**B**). **C)–D)** $S_1 \sim \text{Weibull}$, $S_2 \sim \text{Burr}$, with Δt windows (**C**) and $T_w = 1$ year (**D**). The fixed parameters are: $a_1 = 1.5$, $\tau_1 = 1.3$ years, $\gamma_1 = 30 \text{ years}^{-1}$, $a_2 = 2$, $\tau_2 = 0.75$ years, $\gamma_2 = 40 \text{ years}^{-1}$;

which looks very similar to the formula for $Cov(Q_1, Q_2)$ – this is not surprising since these equations were derived from integrating the autocovariances of A_ν or A_R that only differ by a scaling factor. We state this equation for completeness, and also because it will be used in the next section where we apply our theory to real data.

2.3 Applying our model to industry-wide averages

Obtaining actual operational risk loss data with granular details for a particular institution is extremely difficult due to proprietary reasons. Loss information could reveal vulnerabilities in operations that institutions do not want to publicize, especially to business competitors. The most easily attainable and detailed operational risk loss data we found was provided by **ORX**, an organization that facilitates sharing of actual operational risk losses among its member institutions in a secure and anonymous platform (orx, 2020a). ORX provides information to the public about the total count of loss events and the amount of losses in prior years, as well as the number of member institutions contributing data in a given year (orx, 2020b,c). The cumulative frequency and severity of losses are available by risk categories, see Table 2. We also use the year-to-year covariance of the frequency of losses by risk category shown in Fig 7A. For completeness, we show the year-to-year severity of losses in Fig 7B, but this will not be used (see explanation below). Details on how the ORX data was obtained are outlined in the Materials and methods section.

Important issues to keep in mind: this data provided by ORX is a coarse industry-wide average with contributions from many different institutions, and does not contain the precise times or magnitudes of individual loss events. Thus, the application of our method here is a demonstration, i.e., a proof of principle. With the AMA, external coarse data from ORX is used to merely supplement capital calculations; institutions likely rely on their own internal proprietary data more heavily in their model fitting.

Table 1: **Risk Categories and Abbreviation** The convention used for Operational Risk loss categories are segmented into the 7 categories below. Although the names of each category can vary slightly, the actual descriptions are equivalent; we adopt the naming convention used in ORX (orx, 2020b,c).

Risk Categories	
Abbreviation	Definition
IF	Internal Fraud
EF	External Fraud
EPWS	Employment Practices, Workplace Safety
CPBP	Clients, Products, Business Practices
DPS	Disasters and Public Safety
TIF	Technology and Infrastructure Failure
EDPM	Execution, Delivery and Process Management

2.3.1 Fitting model parameters to ORX data

Although ORX data has some yearly statistics of the severity of losses by risk categories, there is not enough granular detail to estimate the parameters of a given severity distribution. We can only use the ORX data to specify the mean severity *per event* in a given risk category j : μ_{S_j} , the higher order statistics (e.g., variance of loss *per event*) are not accessible.

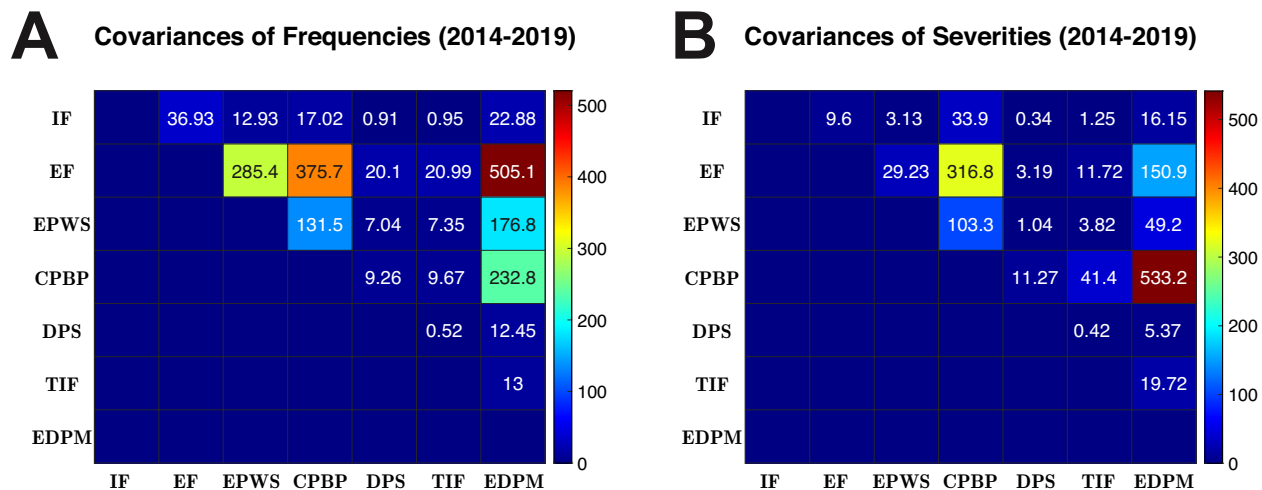


Figure 7: **The year-to-year covariances of ORX data.** **A)** The covariances of the average frequencies per institution by risk category (see Table 1 for definition of abbreviations). **B)** Same as **A** but for average severity per institution (in €-Millions). **Note that (B) is not used in the model fitting**, we provide this for completeness. Excluding diagonal (variances) and lower triangular portion because of symmetry, see Table 2 for the univariate statistics by risk categories.

Table 2: **Statistics by Risk Categories.** Columns show: the average frequency (# events in a year, per institution) and the variances (absent from Fig. 7A), segmented by the 7 risk categories. The last column is the severity (€-Millions) **per event**, which is the only information we have access to for fitting our models to μ_S . The overall average frequency and severity without regard to category are: 514.13 events/year and 321.68 €-Millions/event (resp.). Same ORX data the same source as in Figure 7.

Risk Category	Statistics (over 6 years)		Grand Average
	Frequency Mean (# events per year)	Frequency Var (# events per year) ²	Severity (€-Millions per event)
IF	9.22	1.67	250.91
EF	203.51	815.19	106.23
EPWS	71.25	99.91	98.95
CPBP	93.8	173.16	814.51
DPS	5.02	0.496	153.3
TIF	5.24	0.54	539.31
EDPM	1.26	312.93	288.58

Fortunately, the formula we derived for the covariance of losses in T_w only relies on the mean severities of each event $\mu_{S_{j/k}}$ (via Eq (41)):

$$Cov(Q_j, Q_k) = c_{j,k} \bar{\gamma} \mu_{S_j} \mu_{S_k} a_j a_k \frac{\tau_j \tau_k}{\tau_j + \tau_k} \left[\tau_j \left(T_w + \tau_j (e^{-T_w/\tau_j} - 1) \right) + \tau_k \left(T_w + \tau_k (e^{-T_w/\tau_k} - 1) \right) \right] \Delta t.$$

So fitting our model to ORX data mainly involves the frequency distribution, i.e., fitting $c_{j,k} (j \neq k)$, a_j , τ_j , γ_j , giving a total of 42 parameters to determine with the 7 loss categories (7 different a , τ , γ and 21 input correlations $c_{j,k} (j \neq k)$). We naturally want the mean frequency from the model $\mu_{\nu_j} = a_j \tau_j \gamma_j T_w$ to equal the yearly frequency average from ORX data (Table 2, 1st column), and similarly for the variances (Table 2, 2nd column) and covariances (Fig 7A). Thus our objective is to fit the parameters to the following system:

$$\begin{aligned} a_j \tau_j \gamma_j T_w &= \mu_{\nu_j, ORX} ; \text{ for } j = 1, \dots, 7 \\ a_j^2 \gamma_j \tau_j^2 \left(T_w + \tau_j (e^{-T_w/\tau_j} - 1) \right) &= \sigma_{\nu_j, ORX}^2 ; \text{ for } j = 1, \dots, 7 \\ c_{j,k} \bar{\gamma} a_j a_k \frac{\tau_j \tau_k}{\tau_j + \tau_k} \left[\tau_j \left(T_w + \tau_j (e^{-T_w/\tau_j} - 1) \right) + \tau_k \left(T_w + \tau_k (e^{-T_w/\tau_k} - 1) \right) \right] &= \\ &Cov(\nu_j, ORX, \nu_k, ORX) ; \text{ for } j \neq k \end{aligned}$$

Since the ORX data provides yearly averages, we set $T_w = 1$ year.

Summary of model parameter fitting procedure:

- We set μ_{S_j} equal to the corresponding value in Table 2, right-most column.
- Find 42 parameters ($c_{j,k}$, a_j , τ_j , γ_j) simultaneously using 35 equations from ORX data (7 mean and variances of yearly frequency in first 2 columns of Table 2, 21 covariance frequencies in Fig 7A).

The model fits are very good (Fig 8) despite starting at 1000 random initial conditions using Latin hypercube sampling, see **Materials and methods** sub-section ‘Procedure for fitting model to ORX data’ for details, and Fig. 10 for parameter values. From Fig 8, we see that the solution to the system is not very sensitive to the random initial parameterization. This may not be surprising given that we have an under-constrained system of 35 equations and 42 unknowns (parameters), but note that parameters have constraints: $a_j, \tau_j, \gamma_j > 0$ and $c_{j,k} \in (-1, 1)$. With more granular data, which we do not have access too, there would be more constraints that could certainly effect the quality of the model fits. Whether the solution is unique or not is unknown and beyond the scope of this current study.

2.3.2 Effects of time window on covariance of loss distributions

After finding parameters that capture the frequency distribution well, we can very quickly assess how the covariance $Cov(Q_j, Q_k)$ of the actual loss distributions varies with a large range of time windows; this would usually require time-consuming Monte Carlo simulations

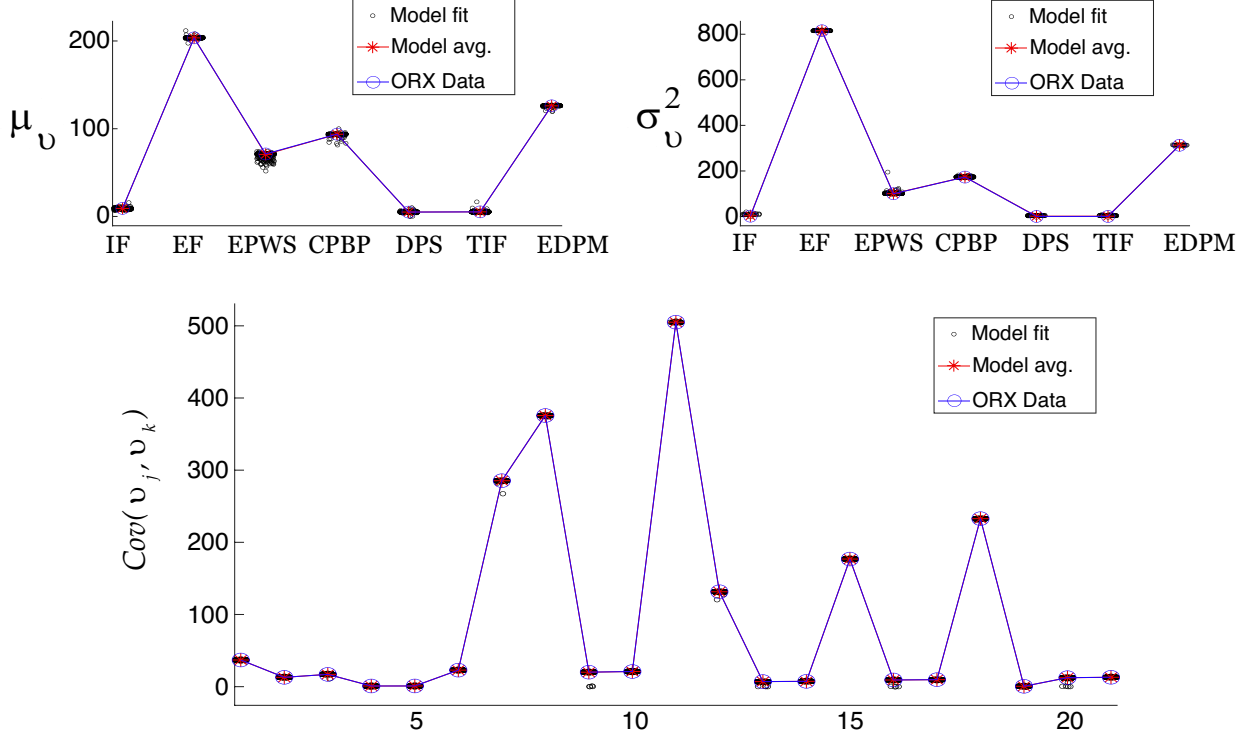


Figure 8: **Fitting model to ORX data.** The 3 yearly frequency statistics we fit: mean μ_ν , variance σ_ν^2 , and covariance $Cov(\nu_j, \nu_k)$. Each of the black dots show the model fit to ORX data at a random starting point for the optimization routine (see **Materials and methods**), the red star is the average of all 1000 fits. In all instances, the model fits the ORX data (blue circles) very well, but recall the system is under-constrained with more parameters (42) than constraints (35). The black circles are jittered horizontally for visual purposes.

but our analytic calculations circumvent and simplify this. We use the average model fit (red stars in Fig 8) as the 42 parameters because there is little deviation among the 1000 model fits, the solution appears quite stable.

The results are summarized in Figure 9. Here we find that the largest covariance of $Q(t)$ is (CPBP, EDPM), and the smallest is with (IF,DPS). We note that the univariate statistics for both the frequency and average severity per event (Table 2) are not at all indicative of which pairs would have the highest covariance, and neither are the covariances of frequencies in Fig 7A (i.e., the largest/smallest covariance in frequencies do not correspond to the largest/smallest covariance of losses in Fig 9). This shows that the correlations of the aggregate loss distributions, specifically which pairs have the largest or smallest correlations, cannot intuited a priori and require proper modeling.

The results in Figure 9 indicate that for all 21 covariances, care must be taken; systems should use a consistent time window, otherwise the covariances can vary by at least a few orders of magnitude when treating daily statistics as yearly statistics.

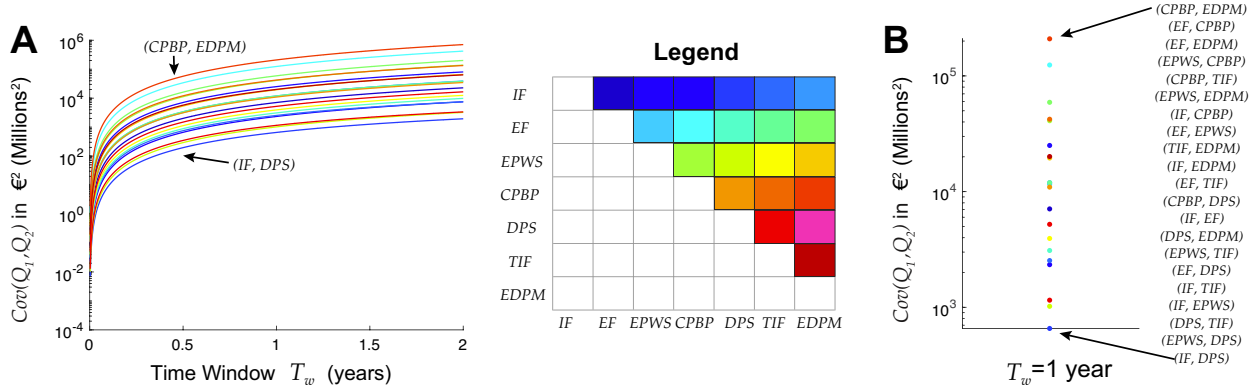


Figure 9: **Covariance of loss distributions fit to ORX data.** **A)** The resulting $Cov(Q_j, Q_k)$ for all 21 pairs as a function of time window T_w (log scale on vertical axes). The statistics can vary a few orders of magnitude or more for these times. The legend is shown on the right. **B)** Shows the order of smallest and largest covariance pairs, setting $T_w = 1$ year for exposition purposes. The ordering does not change as T_w varies.

3 Discussion

We present, develop and apply a framework to mathematically account for how the correlation of loss distributions could vary when data are collected and/or processed on different time scales. Specifically, we use a dynamic stochastic differential equation model for the frequency distribution of Operational Risk loss events. This model is a generalization of commonly used homogeneous Poisson Process frequency model, capturing time-varying changes in the statistics of the frequency and equipped with temporal correlations that do not exist in homogeneous Poisson Process models. The frequency distribution model contains these complexities yet has only a few parameters and is amenable to mathematical calculations that result in relatively accurate formulas. This paper provides detailed mathematical calculations and thorough comparisons with Monte Carlo simulations with a large range of parameters. However, the method and overall framework we have outlined and implemented where the variance/covariance in arbitrary time windows is obtained from integrating the autocovariance/cross-covariance multiplied by $(T_w - |t|)$ (Eqs (5), (18)), is general and does not require the specific inhomogeneous Poisson Process model for the frequency distribution we introduced. This method can be applied to any frequency distribution model as long as the auto/cross-covariance can be calculated.

Our application of methods relating the cumulative loss statistics to the statistics in smaller time windows is inspired by the successful usage in other disciplines (signal processing (Kay, 1993), computational neuroscience (Lindner et al., 2005; Shea-Brown et al., 2008; Litwin-Kumar et al., 2011, 2012; Barreiro and Ly, 2017, 2018)), but the models we use here are specific to Operational Risk, thus yielding novel formulas and applications.

The loss time series have temporal correlation within a risk category *and* correlation across risk categories, so we use conventional Monte Carlo simulations with a time dis-

cretization. The time discretization is advantageous for obtaining the simulated auto/cross-covariance function needed in our theory (recall Figs 4, 5A,B). Whether it is possible to simulate just the event times without discretizing time (i.e., Gillespie algorithm) and rescale to equivalent pathwise deterministic Markov processes is not obvious to us; we believe this would require new methods and is beyond the scope of this study.

We demonstrate in principle how our loss distribution model could be fit to actual operational risk data. Since the data was provided by an exchange (ORX) with only industry-wide averages from many different institutions that vary in size, scope, objective, etc., the details of our application and results would likely be very different in practice. The ORX data was very coarse, lacking granular details of loss events that individual institutions might access to, including time of occurrence and magnitude. Nevertheless, the ORX data contained information about the average severity of losses per event, segmented by 7 common risk categories, as well as the year-to-year frequency of events from 2014–2019. Although not meant to be a definitive model to supplant the status quo, we use the model to estimate the covariances of aggregate loss distributions. Moreover, our mathematical calculations enabled us to quickly assess how the covariances of the losses change with different time windows, showing that if institutions are not careful in their systems, e.g., they are not using the same time windows to estimate covariances (especially with risk categories with inherently different time-scales) that feed into copula calculations, the results of their capital calculations could be significantly inaccurate.

We close with some remarks about applying our method to actual data. Institutions use their proprietary internal data that has significantly more details of individual loss events, so they can certainly have more data constraints in their model fitting than what we demonstrated here. It is natural to have an over-constrained system in fitting our model to an institution’s data. Individual institutions also do not necessarily use these specific seven risk categories provided by ORX (Table 1), they may have more (and different) risk categories that could each be modeled by a different frequency and severity model. In our specific demonstration, we did not normalize the magnitudes of the ORX data across risk categories; it may be desirable to model relative percent differences versus capturing vast differences across risk categories. Sensitivity analyses of model fits are a key component: with our model, the mathematical formulas used to estimate (co-)variances should be varied (perhaps with Monte Carlo simulations, and also setting the correlations to extreme values of ± 1) to assess how capital calculations change. The merits of our model applied to a specific institution and their data are to be determined, but note that all model components in this paper, including figures and tables, are freely available on GitHub.

4 Materials and methods

See GitHub page <https://github.com/chengly70/OperationalRisk/> for freely available code simulating the models in this paper, including comparisons to Monte Carlo simulations, implementation of analytic formulas, processing of freely available ORX data, model fitting to ORX data, etc.

For the severity distribution we consider several commonly used parametric distributions $f_S(x)$ (Chernobai et al., 2008):

$$f_S(x) = \frac{1}{\Gamma(\alpha)\beta} \left(\frac{x}{\beta}\right)^{\alpha-1} \exp\left(-x/\beta\right), \text{ for } x > 0; \alpha, \beta > 0, \text{ Gamma} \quad (21)$$

$$f_S(x) = \frac{1}{x\sqrt{2\pi}\sigma} \exp\left(-\frac{(\log(x) - \mu)^2}{2\sigma^2}\right), \text{ for } x > 0; \mu \in \mathbb{R}, \sigma > 0, \text{ Lognormal} \quad (22)$$

$$f_S(x) = \frac{1}{\sigma} \left(1 + k\frac{x}{\sigma}\right)^{-1-1/k}, \text{ for } x > 0, \text{ GPD} \quad (23)$$

$$f_S(x) = \frac{b}{a} \left(\frac{x}{a}\right)^{b-1} \exp\left(-\left(\frac{x}{a}\right)^b\right), \text{ for } x > 0; b > 0; a > 0, \text{ Weibull} \quad (24)$$

$$f_S(x) = \frac{\frac{kx}{\alpha} \left(\frac{x}{\alpha}\right)^{c-1}}{\left(1 + \left(\frac{x}{\alpha}\right)^c\right)^{k+1}}, \text{ for } x > 0; \alpha > 0; c > 0; k > 0, \text{ Burr} \quad (25)$$

The statistics for these common distributions are shown in Table 3.

Table 3: Severity distribution family and statistics. Here $\Gamma(x) = \int_0^\infty z^{x-1}e^{-z} dz$ and $B(x, y) = \Gamma(x)\Gamma(y)/\Gamma(x+y)$. To insure the mean and variances are finite, in **GPD** we have $0 \leq k < \frac{1}{2}$, in **Burr** we have $k > \frac{2}{c}$.

Distribution	Mean $\mathbb{E}[S] = \mu_S$	Variance $\mathbb{E}[S^2] - \mathbb{E}[S]^2 = \sigma_S^2$	Allowable Parameters
Gamma	$\alpha\beta$	$\alpha\beta^2$	$\alpha, \beta > 0$
Lognormal	$\exp(\mu + \sigma^2/2)$	$(e^{\sigma^2} - 1)e^{2\mu + \sigma^2}$	$\sigma > 0$
GPD	$\frac{\sigma}{(1-k)}$	$\frac{\sigma^2}{(1-k)^2(1-2k)}$	$\sigma > 0$ and $0 \leq k < \frac{1}{2}$
Weibull	$a\Gamma\left(1 + \frac{1}{b}\right)$	$a^2\Gamma\left(1 + \frac{2}{b}\right) - a^2\left(\Gamma\left(1 + \frac{1}{b}\right)\right)^2$	$a, b > 0$
Burr	$k\alpha B\left(k - \frac{1}{c}, 1 + \frac{1}{c}\right)$	$k\alpha^2 B\left(k - \frac{2}{c}, 1 + \frac{2}{c}\right) - (k\alpha)^2 B\left(k - \frac{1}{c}, 1 + \frac{1}{c}\right)^2$	$\alpha, c, k > 0$ and $k > \frac{2}{c}$

4.1 Calculations for a single inhomogeneous Poisson Process frequency model

Recall $R(t) = S * I(t)$, with $P(I(t) = 1) = \nu(t)\Delta t$ where the time points t are spaced a part by Δt , and where $\nu(t)$ is the probability per unit time of a loss event occurring. The model for $\nu(t)$ is:

$$\tau \frac{d}{dt} \nu(t) = -\nu(t) + \tau a \sum_k \delta(t - t_k) \quad (26)$$

where t_k are random points drawn from a homogeneous Poisson Process with rate γ , a is the jump size of $\nu(t)$ at times t_k , and τ is the time-scale that determines how fast $\nu(t)$ decays to 0 in the absence of random jumps at t_k .

The statistics of $\nu(t)$ are calculated by a stochastic integral formulation of the equation:

$$\nu(t) = a \int_0^\infty D(t-t') e^{-\frac{t'}{\tau}} dt'$$

where $D(t) = \sum_k \delta(t-t_k)$, and $\mathbb{E}[D(t)] = \gamma$. Taking the expected value of this equation and recognizing the only source of randomness on the rhs is D , we get:

$$\mathbb{E}[\nu(t)] = a \int_0^\infty \mathbb{E}[D(t-t')] e^{-\frac{t'}{\tau}} dt' = a\gamma\tau.$$

Thus we have:

$$\mathbb{E}[R] = \mathbb{E}_\nu[\mathbb{E}[R|\nu]] = \mathbb{E}_{\nu(t)}[\mu_S \nu(t) \Delta t] = \mu_S \Delta t \mathbb{E}_{\nu(t)}[\nu(t)] = \mu_S (a\gamma\tau \Delta t). \quad (27)$$

For the variance we need the 2nd moment of $\nu(t)$.

$$\nu(t)^2 = a^2 \int_0^\infty \int_0^\infty D(t-u) D(t-v) e^{-\frac{u}{\tau}} e^{-\frac{v}{\tau}} du dv. \quad (28)$$

Using this property of homogeneous Poisson Processes:

$$\mathbb{E}[D(t-u)D(t-v)] = (a\gamma)^2 + \gamma\delta(u-v),$$

we get the second moment of $\nu(t)$ is:

$$\mathbb{E}[\nu(t)^2] = (a\gamma\tau)^2 + a^2\gamma \int_0^\infty e^{-\frac{2v}{\tau}} dv = (a\gamma\tau)^2 + \frac{a^2\gamma\tau}{2}. \quad (29)$$

The variance of $\nu(t)$ is:

$$Var(\nu(t)) = \frac{a^2\gamma\tau}{2} \quad (30)$$

The autocovariance $\mathbb{E}[\nu_{t'}\nu_{t'+t}] - \mathbb{E}[\nu(t)]^2$ is similarly calculated by replacing $D(t-u)$ with $D(t'+t-u)$ in Eq (28):

$$A_{\nu(t)}(t) = \frac{a^2\gamma\tau}{2} e^{-|t|/\tau} \quad (31)$$

Since the second moment of R is:

$$\mathbb{E}_\nu[\mathbb{E}[R^2|\nu(t)]] = \mu_{S^2} \Delta t \mathbb{E}_{\nu(t)}[\nu(t)] = \mu_{S^2} (a\tau\gamma\Delta t),$$

the variance of R is:

$$\sigma_R^2 = \mu_{S^2} (a\tau\gamma\Delta t) - (\mu_S a\tau\gamma\Delta t)^2 \quad (32)$$

For cumulative losses in larger time windows, the statistics are calculated similarly, with:

$$\mu_Q = \sum \mathbb{E}[R] = n\Delta t (a\gamma\tau\mu_S) = T_w a\gamma\tau\mu_S \quad (33)$$

To obtain the autocovariance of R , we leverage that fact that the support (where $R > 0$ in time) is the same as the realization of $\nu(t)$, so the temporal structure of R and $\nu(t)$ are identical, with the only difference being the magnitudes. So the autocovariance of R must also be of similar form to $A_{\nu(t)}$ except we have $A_R(t = 0) = \sigma_R^2$:

$$A_R(t) = \sigma_R^2 \frac{e^{-|t|/\tau}}{\Delta t}. \quad (34)$$

With the calculation of $A_R(t)$ in hand, we use

$$\sigma_Q^2 = \int_{-T_w}^{T_w} A(t) (T_w - |t|) dt$$

(repeat of equation (5)) to get an approximation to the variance of cumulative losses in a time window T_w :

$$\sigma_Q^2 = \int_{-T_w}^{T_w} A_R(t) (T_w - |t|) dt = 2 \frac{\sigma_R^2}{\Delta t} \tau (T + \tau(e^{-T/\tau} - 1)). \quad (35)$$

This approximation assumes $A(t)$ suffices to capture σ_Q^2 .

4.2 Calculations for two loss time series

To generalize the theory and calculations from the prior section, we consider the cross-covariance function of $CC_{\nu}(t) := \mathbb{E}[\nu_1(t'+t)\nu_2(t')] - \mathbb{E}[\nu_1]\mathbb{E}[\nu_2]$; note that $CC_{\nu}(t) \neq CC_{\nu}(-t)$, unlike with the autocovariance function where $A(t) = A(-t)$ for both R and $\nu(t)$. The analogous equation to Eq. (28) is:

$$\nu_1(t')\nu_2(t'+t) = a_1 a_2 \int_0^{\infty} \int_0^{\infty} D_1(t'+t-u) D_2(t'-v) e^{\frac{-u}{\tau_1}} e^{\frac{-v}{\tau_2}} du dv. \quad (36)$$

where $D_j(t) = \sum_{k_j} \delta(t - t_{k_j})$. Since

$$\mathbb{E}[D_1(t'+t-u)D_2(t'-v)] - \gamma_1\gamma_2 = c\bar{\gamma}\delta(t-u+v)$$

by construction, we take the expected value of Eq. (36), using similar calculations as before (cf. Eq. (29)) to get:

$$CC_{\nu}(t) = c\bar{\gamma}a_1a_2 \frac{\tau_1\tau_2}{\tau_1 + \tau_2} \begin{cases} e^{-t/\tau_1}, & \text{if } t \geq 0 \\ e^{-|t|/\tau_2}, & \text{if } t < 0 \end{cases}. \quad (37)$$

We apply the same arguments as before when deriving $A_R(t)$ (Eq. (34)): since $R(t)$ and D_j have the same temporal support, the cross-covariance functions must be of a similar form.

We first derive the point-wise covariance for the losses in small windows Δt : $Cov(R_1, R_2)$ and set this to $CC_R(t=0)$ to get:

$$CC_R(t) = \frac{Cov(R_1, R_2)}{\Delta t} \begin{cases} e^{-t/\tau_1}, & \text{if } t \geq 0 \\ e^{-|t|/\tau_2}, & \text{if } t < 0 \end{cases} \quad (38)$$

To derive $Cov(R_1, R_2)$, we employ similar methods for σ_R^2 (Eq. 32):

$$\begin{aligned} \mathbb{E}[R_1(t)R_2(t)] &= \mathbb{E}_\nu \left[\mathbb{E}[R_1 R_2 | \nu] \right] \\ &= \mu_{S_1} \mu_{S_2} \mathbb{E}_\nu [\nu_1 \nu_2] (\Delta t)^2 \\ &= \mu_{S_1} \mu_{S_2} \left(c\bar{\gamma} a_1 a_2 \frac{\tau_1 \tau_2}{\tau_1 + \tau_2} (\Delta t)^2 + (a_1 \tau_1 \gamma_1 \Delta t)(a_2 \tau_2 \gamma_2 \Delta t) \right), \end{aligned} \quad (39)$$

to get:

$$Cov(R_1, R_2) = \mu_{S_1} \mu_{S_2} c\bar{\gamma} a_1 a_2 \frac{\tau_1 \tau_2}{\tau_1 + \tau_2} (\Delta t)^2. \quad (40)$$

Using the same method as before to relate the autocovariance of R to the variance of cumulative losses in larger time windows T_w , we relate the cross-covariance function to the covariance of cumulative losses in T_w :

$$\begin{aligned} Cov(Q_1, Q_2) &= \int_{-T_w}^{T_w} CC_R(t) (T_w - |t|) dt \\ &= Cov(R_1, R_2) \frac{\tau_1 (T_w + \tau_1 (e^{-T_w/\tau_1} - 1)) + \tau_2 (T_w + \tau_2 (e^{-T_w/\tau_2} - 1))}{\Delta t} \\ Cov(Q_1, Q_2) &= c\bar{\gamma} \mu_{S_1} \mu_{S_2} a_1 a_2 \frac{\tau_1 \tau_2}{\tau_1 + \tau_2} \left[\tau_1 (T_w + \tau_1 (e^{-T_w/\tau_1} - 1)) + \tau_2 (T_w + \tau_2 (e^{-T_w/\tau_2} - 1)) \right] \Delta t \end{aligned} \quad (41)$$

4.3 Details for Obtaining ORX Data

The total frequency and severity of operational risk losses from the consortium of all banks, segmented by risk categories, is directly reported in the ORX Annual Banking Lost Report (orx, 2020b) (see Tables 4–5). There are however two important aspects of the data that we must address so that it is in a usable form (i.e., yearly data for Banking losses only): i) the data is cumulative over 6 years (2014–2019), ii) the data combines all business types (Banking, Trading and Investments, Corporate Items, Other) while our application concerns only Banking losses.

Starting with Tables 4–5, we approximate the yearly frequency and severity by taking a fraction (73% for frequency, 56% for severity) of the yearly amounts reported on page 6 of orx (2020b) (see Table 6). Note that the percentages (73%, 56%) are the reported fractions from Bank losses alone; see pages 10 and 12, respectively, in orx (2020b). With an approximation

Table 4: Extracted data of frequency of events with risk category proportions, from page 11 of orx (2020b). We calculated the row ‘% of Total from Bank Loss’ as a proportion of the total, the last row is from page 10 of orx (2020b).

	IF	EF	EPWS	CPBP	DPS	TIF	EDPM	Totals
Retail Banking	4561	100361	35026	39991	2509	2116	51352	235916
Private Banking	140	1671	1794	3268	23	110	3947	10953
Commercial Banking	327	8949	2033	7891	206	631	13462	33499
Totals	5028	110981	38853	51150	2738	2857	68761	280368
% of Total from Bank Loss	2%	40%	14%	18%	1%	1%	25%	
% Bank Losses to Gross	73%							

Table 5: Extracted data of severity of losses (€-Million) with risk category proportions, from page 13 of orx (2020b). We calculated the row ‘% of Total from Bank Loss’ as a proportion of the total, the last row is from page 12 of orx (2020b).

	IF	EF	EPWS	CPBP	DPS	TIF	EDPM	Totals
Retail Banking	950	7045.2	3394.7	26504.3	389.7	844.4	13655.6	52783.9
Private Banking	161.1	304.4	233.8	2456.2	2.1	27.6	886.6	4071.8
Commercial Banking	158.4	4514	240	12962	30.3	678.4	5425.1	24008.2
Totals	1269.5	11863.6	3868.5	41922.5	422.1	1550.4	19967.3	80863.9
% of Total from Bank Loss	2%	15%	5%	52%	1%	2%	25%	
% Bank Losses to Gross	56%							

for each of the 6 years, we then use the computed percentages (row 5 of Tables 4–5) to distribute the loss data by risk category. The final step is to divide the loss data by the number of contributing bank institutions (see bottom row of Table 6), to get yearly data of realized losses from the average institution.

Table 6: Extracted frequency and severity data by year (page 6 of orx (2020b)) that includes all business types: Banking, Trading and Investments, Corporate Items, Others. The total number of institutions reporting by year (bottom row) is from page 4 of orx (2020b)).

Year	2014	2015	2016	2017	2018	2019
Total # Events	65766	69519	65797	63491	59642	59437
Total Losses (€-Billion)	37.6	25.1	28.1	20	17.6	15.8
Total # Institutions	80	85	92	96	97	100

4.4 Procedure for fitting model to ORX data

Recall the system of 35 equations is:

$$\begin{aligned}
 a_j \tau_j \gamma_j T_w &= \mu_{\nu_j, ORX} ; \text{ for } j = 1, \dots, 7 \\
 a_j^2 \gamma_j \tau_j^2 \left(T_w + \tau_j (e^{-T_w/\tau_j} - 1) \right) &= \sigma_{\nu_j, ORX}^2 ; \text{ for } j = 1, \dots, 7
 \end{aligned}$$

$$c_{j,k}\bar{\gamma}a_ja_k\frac{\tau_j\tau_k}{\tau_j+\tau_k}\left[\tau_j\left(T_w+\tau_j(e^{-T_w/\tau_j}-1)\right)+\tau_k\left(T_w+\tau_k(e^{-T_w/\tau_k}-1)\right)\right]=$$

$$Cov(\nu_{j,ORX},\nu_{k,ORX}); \text{ for } j \neq k$$

the 42 unknowns are $(a_j, \tau_j, \gamma_j, c_{j,k}) =: \vec{x}$. The left-hand side are statistics from the model X_{mod} and the right-hand side are the statistics from ORX data.

We use MATLAB's `fmincon` optimization routine to find parameters that minimize the following objective function, i.e., the l_1 norm of data and model:

$$\min_{\vec{x}} \sum_{j=1}^7 \left(\left| \mu_{\nu_j,mod} - \mu_{\nu_j,ORX} \right| + \left| \sigma_{\nu_j,mod}^2 - \sigma_{\nu_j,ORX}^2 \right| \right) + \sum_{j < k} |Cov(\nu_{j,mod}, \nu_{k,mod}) - Cov(\nu_{j,ORX}, \nu_{k,ORX})|$$
(42)

We do not know if there exists a unique solution to this problem, so we use `fmincon` with 1000 random initial parameterizations \vec{x}_0 using Latin hypercube sampling with:

$$\begin{aligned} a_j &\sim Unif(0, 15) \\ \tau_j &\sim Unif(0, 2) \\ \gamma_j &\sim Unif(0, 40) \\ c_{j,k} &\sim Unif(-1, 1) \end{aligned}$$

These particular distributions were arbitrarily chosen, except for the input correlation because $-1 < c_{j,k} < 1$ and the constraint that $a, \tau, \gamma > 0$. The upper bounds for (a, τ, γ) are within the range of average number of events per year across the 7 risk categories (see Table 2).

The code to implement all of this is freely available at <https://github.com/chengly70/OperationalRisk/> in function `MORE_fitFreq_Parms.m`.

5 Appendix: Homogenous Poisson Process

We first consider a simple time series where the frequency distribution is given by a Poisson Process with rate ν_r events/time, and an independent severity distribution f_S . Note that despite the simplicity of this model, it is still commonly used as a default model, especially for loss categories without a lot of data, because it is relatively transparent (Chernobai et al., 2008). We present the calculation of second order statistics of the whole time series for a given loss category. For each risk type and a given period, operational losses are represented by a time series R_j , where j indexes a time interval of size Δt (assumed to be small enough so that at most one operational loss event can occur); this particular aggregate loss distribution is commonly referred to as a marked Poisson Process (Last and Penrose, 2017).

The probability of a loss event at a given time bin $(t, t + \Delta t)$ is $\nu_r \Delta t$ and each time bin is independent. To derive desired first and second order statistics, we use the PDF of R , where

$$P(I = 1) = \nu_r \Delta t, \quad P(I = 0) = 1 - \nu_r \Delta t. \tag{43}$$

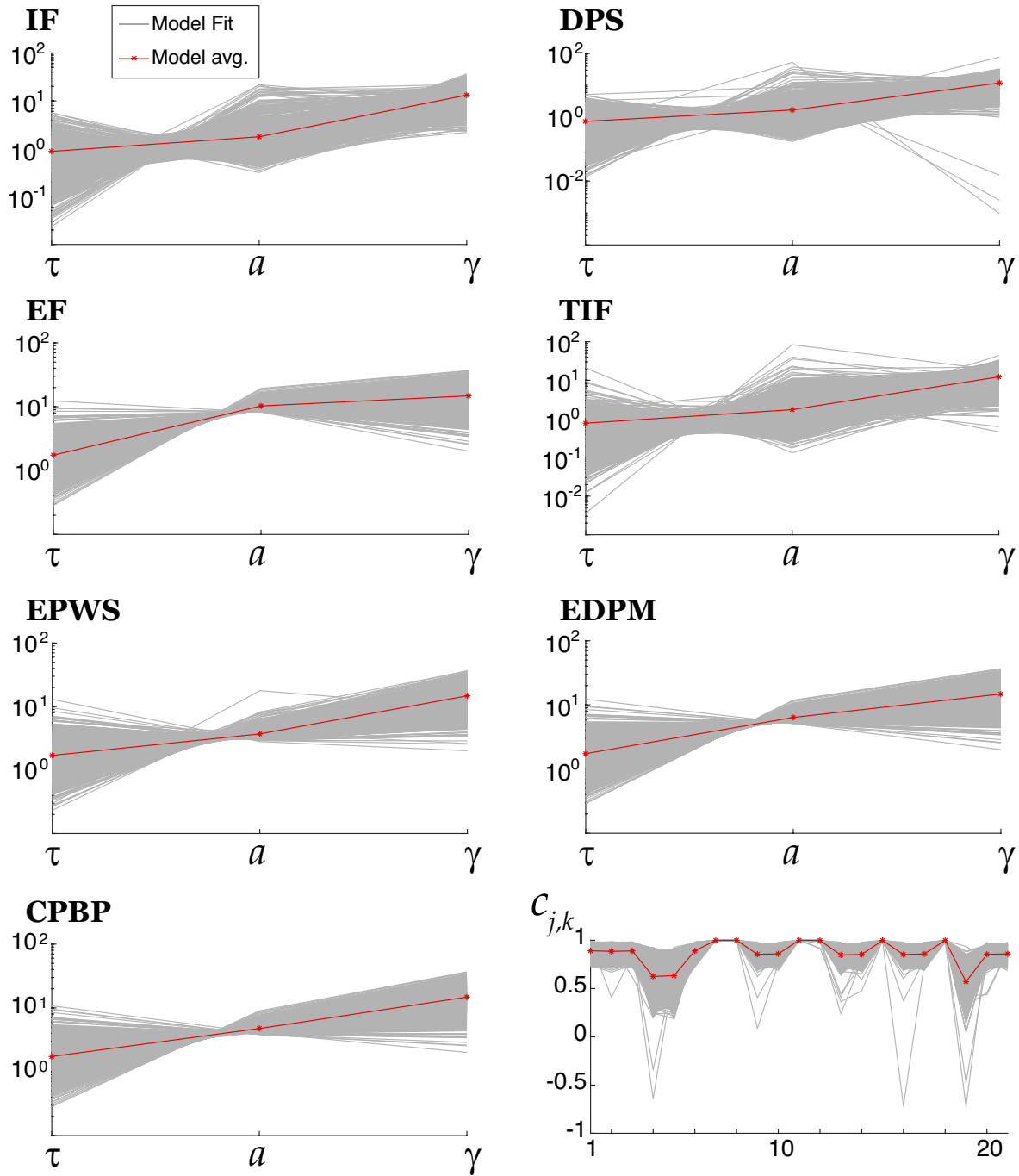


Figure 10: **Details of 42 parameter values fit to ORX data.** Showing all 1000 model fits (gray lines) with lines connecting a particular random parameterization, and the model averages (red stars). The parameters (τ, a, γ) are segmented by the 7 risk categories, all 21 input correlations ($c_{j,k}$) are in lower right panel.

The mean is:

$$\begin{aligned}
\mu_R &= \mathbb{E}[IS] = \mathbb{E}[I]\mathbb{E}[S] \\
&= 0 * P(I = 0)\mathbb{E}[S] + 1 * P(I = 1)\mathbb{E}[S] = 1 * \nu_r \Delta t \mu_S \\
\Rightarrow \mu_R &= (\nu_r \Delta t) \mu_S
\end{aligned} \tag{44}$$

where μ_S is the mean of the chosen severity distribution. The second moment of R is:

$$\mathbb{E}[R^2] = 0^2 * (1 - \nu_r \Delta t) + 1^2 * (\nu_r \Delta t) \mathbb{E}[S^2] = (\nu_r \Delta t) \mu_{S^2}$$

so the variance is:

$$\sigma_R^2 = (\nu_r \Delta t) \mu_{S^2} - (\nu_r \Delta t \mu_S)^2 \tag{45}$$

5.0.1 Cumulative Loss Statistics in Arbitrary Time Windows

For the purposes of aggregating capital over different time horizons (i.e., yearly capital assessment is a regulatory requirement (Bank For International Settlements, 2014; Chernobai et al., 2008)), we consider cumulative losses over different time windows to understand how this practice of using different time windows might effect the statistics. Development of methods to capture cumulative losses in arbitrary time windows may also help institutions handle certain operational loss categories that occur infrequently or where data quality is bad and thus data is unreliable. Recall that R is the loss in small time bin Δt , the cumulative losses in a time window of length T_w that contains $n := T_w/\Delta t$ time bins is:

$$Q_l = \sum_{j=1}^n R_{j+(l-1)n} \tag{46}$$

where the subscript l denotes the l^{th} window of length T_w . The mean is:

$$\mu_Q = \sum \mathbb{E}[R] = n \Delta t (\nu_r \mu_S) = T_w \nu_r \mu_S \tag{47}$$

With a homogeneous Poisson Process model, each of the R 's are independent, making the calculation of the variance simpler because the covariance terms are 0:

$$\begin{aligned}
\sigma_Q^2 &= \sum Var(R_j) + 2 \sum_{j < k} Cov(R_j, R_k) = n [(\nu_r \Delta t) \mu_{S^2} - (\nu_r \Delta t \mu_S)^2] \\
&= T_w \nu_r (\mu_{S^2} - \nu_r \Delta t (\mu_S)^2)
\end{aligned} \tag{48}$$

5.0.2 Relationship between autocovariance and Q

The autocovariance function is common tool to quantify the temporal dynamics of a time series; here we define it as:

$$A(t) = \mathbb{E}_{t'} [R_{t'+t} R_{t'}] - \mathbb{E}_{t'} [R_{t'}]^2 \tag{49}$$

$A(t)$ specifies how correlated (or degree of co-variability) two points separated by time t are. Note that $A(t = 0) = \sigma_T^2$ is the (point-wise) variance calculated from samples at each Δt . The autocovariance has a nice relationship with the cumulative cum in a window of length T_w whenever the time series satisfies stationarity (Kay, 1993):

$$\sigma_Q^2 = \int_{-T_w}^{T_w} A(t) (T_w - |t|) dt \quad (50)$$

Indeed, we can use this equation to derive equation (48); note that the Autocovariance function of R with a Poisson Process frequency distribution and independent severity distribution is simply:

$$A(t) = \sigma_R^2 \delta(t) = \sigma_R^2 \frac{1}{\Delta t}. \quad (51)$$

Substituting this into equation (5), we get:

$$\sigma_Q^2 = \sigma_R^2 (T_w - |t|) \Big|_{t=0} = \sigma_R^2 T_w = (\nu_r \mu_s^2 - (\nu_r \mu_s)^2 \Delta t) T_w = T_w \nu_r (\mu_S^2 - \nu_r \Delta t (\mu_S)^2),$$

which is the same as equation (48).

This property will be subsequently used to determine variance in more complex cases, such as when we consider models with time-dependent probability of loss events.

5.0.3 Summary of Homogeneous Poisson Process results

Fig 11 demonstrates the accuracy of our analytic calculations for a wide variety of severity distribution parameters. The dark blue stars are the loss statistics in small time windows Δt calculated by Monte Carlo, while the analytic formulas are solid black curves. The light blue stars are the loss statistics in a larger time window ($T_w = 1$ year here), following the dark/light blue coloring convention in Fig 1. Overall we see that our formulas are very accurate (see legend for further details).

The formulas we derived for the mean and variance of aggregate loss distributions assuming a homogeneous Poisson Process frequency distribution and independent severity distribution (Eq (44), (45), (47), (48)) are straightforward calculations but have scarcely been reported. This could be due to a number of factors, including: focus on tail-end loss distribution, desire to keep methods proprietary, reliance on Monte Carlo simulations, lack of temporal dependence, etc. Nevertheless, our work shows analytic calculations are possible for this common frequency distribution model and very accurate.

Declaration of Interest

The authors report no conflicts of interest. The authors alone are responsible for the content and writing of the paper.

References

- (2020 (accessed August 25, 2020)a). ORX. <https://managingrisktogether.orx.org/about>.
- (2020 (accessed August 25, 2020)b). ORX. <https://managingrisktogether.orx.org/loss-data/annual>
- (2020 (accessed August 25, 2020)c). ORX. <https://managingrisktogether.orx.org/orx-news/monthly>
- Afonso, G. M., A. Mihov, F. Curti, et al. (2019). Coming to terms with operational risk. (20190107), <https://ideas.repec.org/p/fip/fednls/87301.html>.
- Bank For International Settlements (2014). Basel committee on banking supervision. operational risk – revisions to the simpler approaches. ISBN 978-92-9131-869-8, <https://www.bis.org/publ/bcbs291.pdf>.
- Barreiro, A. and C. Ly (2017). When do correlations increase with firing rates in recurrent networks? PLoS Computational Biology 13, e1005506. DOI: 10.1371/journal.pcbi.1005506.
- Barreiro, A. and C. Ly (2018). Investigating the correlation-firing rate relationship in heterogeneous recurrent networks. Journal of Mathematical Neuroscience 8, 8. DOI: 10.1186/s13408-018-0063-y.
- Chernobai, A. S., S. T. Rachev, and F. J. Fabozzi (2008). Operational risk: a guide to Basel II capital requirements, models, and analysis, Volume 180. John Wiley & Sons.
- De Fontnouvelle, P., D. Jesus-Rueff, J. S. Jordan, E. S. Rosengren, et al. (2003). Using loss data to quantify operational risk. Federal Reserve Bank of Boston, <http://dx.doi.org/10.2139/ssrn.395083>. DOI: 10.2139/ssrn.395083.
- Hawkes, A. G. (1971). Spectra of some self-exciting and mutually exciting point processes. Biometrika 58(1), 83–90. DOI: 10.1093/biomet/58.1.83.
- Hawkes, A. G. (2018). Hawkes processes and their applications to finance: a review. Quantitative Finance 18(2), 193–198. DOI: 10.1080/14697688.2017.1403131.
- Jiřina, M. (2011). Trends in banks operational risk losses. In Proceedings of the 10th WSEAS international conference on E-Activities, pp. 95–100. World Scientific and Engineering Academy and Society (WSEAS). <https://dl.acm.org/doi/abs/10.5555/2183339.2183354>.
- Kay, S. M. (1993). Fundamentals of statistical signal processing. Prentice Hall PTR.
- Last, G. and M. Penrose (2017). Lectures on the Poisson process, Volume 7. Cambridge University Press.
- Lindner, B., B. Doiron, and A. Longtin (2005). Theory of oscillatory firing induced by spatially correlated noise and delayed inhibitory feedback. Physical Review E 72(6), 061919. DOI: 10.1103/PhysRevE.72.061919.

- Litwin-Kumar, A., M. J. Chacron, and B. Doiron (2012). The spatial structure of stimuli shapes the timescale of correlations in population spiking activity. PLoS Comput Biol 8(9), e1002667. DOI: 10.1371/journal.pcbi.1002667.
- Litwin-Kumar, A., A.-M. M. Oswald, N. N. Urban, and B. Doiron (2011). Balanced synaptic input shapes the correlation between neural spike trains. PLoS Comput Biol 7(12), e1002305. DOI: 10.1371/journal.pcbi.1002305.
- McNeil, A. J., R. Frey, and P. Embrechts (2015). Quantitative risk management: concepts, techniques and tools-revised edition. Princeton university press.
- Shea-Brown, E., K. Josić, J. De La Rocha, and B. Doiron (2008). Correlation and synchrony transfer in integrate-and-fire neurons: basic properties and consequences for coding. Physical review letters 100(10), 108102. DOI: 10.1103/PhysRevLett.100.108102.

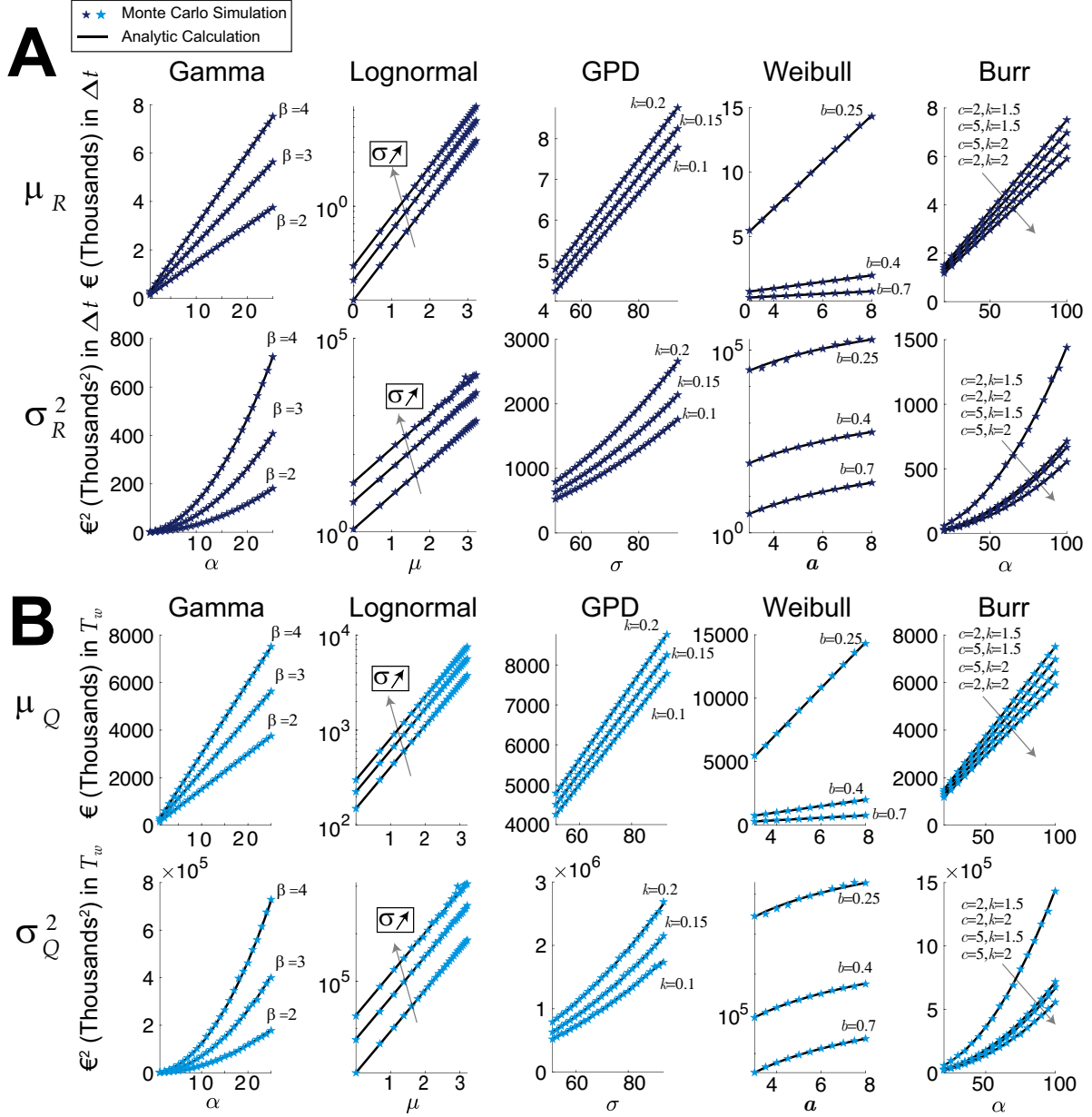


Figure 11: **Accurate analytic formulas for homogeneous PP frequency model.** Comparing the mean and var of R and Q following format of Figure 2 but with a homogeneous Poisson Process frequency distribution ($\nu_r = 75$ events/year) for common severity distributions (see Table 3). Note that Table 2 shows that this average frequency is typical in industry-wide reporting. **A**) Mean μ_R and variance σ_R^2 of aggregate loss distribution in small windows $\Delta t = 0.001$ in time units of years (≈ 0.365 day), with Monte Carlo simulations in stars (Eq. (3)) and analytic formulas in solid curves (Eq. (44) and (45)). **B**) Mean μ_Q and variance σ_Q^2 of cumulative losses in large time windows $T_w = 1$ year, with Monte Carlo simulations in stars (Eq. (46)) and calculations with solid curves (Eq. (47) and (48)).